Downloaded from orbit.dtu.dk on: Apr 01, 2019

DTU Library

Optimal control of a high-frequency class-D amplifier

Dahl, Nicolai Jerram; Iversen, Niels Elkjær; Knott, Arnold; Andersen, Michael A. E.

Published in:
Journal of the Audio Engineering Society

Link to article, DOI:
10.17743/jaes.2017.0046

Publication date:
2018

Document Version
Peer reviewed version

Link back to DTU Orbit

Citation (APA):
Dahl, N. J., Iversen, N. E., Knott, A., & Andersen, M. A. E. (2018). Optimal control of a high-frequency class-D amplifier. Journal of the Audio Engineering Society, 66(1-2), 34-43. DOI: 10.17743/jaes.2017.0046

General rights
Copyright and moral rights for the publications made accessible in the public portal are retained by the authors and/or other copyright owners and it is a condition of accessing publications that users recognise and abide by the legal requirements associated with these rights.

- Users may download and print one copy of any publication from the public portal for the purpose of private study or research.
- You may not further distribute the material or use it for any profit-making activity or commercial gain
- You may freely distribute the URL identifying the publication in the public portal

If you believe that this document breaches copyright please contact us providing details, and we will remove access to the work immediately and investigate your claim.

Optimal Control of a High Frequency Class-D Amplifier*

Nicolai Dahl, *AES Student Member* **Niels Iversen,** *AES Student Member* **Arnold Knott,** *AES Member* **Michael Andersen,** *AES Member*
(nicolai@jerram.dk) (neiv@elektro.dtu.dk) (akn@elektro.dtu.dk) (mea@elektro.dtu.dk)

Technical University of Denmark, Kgs. Lyngby, Denmark

Control loops have been used with switch-mode audio amplifiers to improve the sound quality of the amplifier. Because these amplifiers use a high frequency modulation, precautions in the controller design must be taken. Further, the quality factor of the output filter can have a great impact on the controller's capabilities to suppress noise and track the audio signal. In this paper, design methods for modern control are presented. The control method proves to easily overcome the challenge of designing a good performing controller when the output filter has a high quality factor. The results show that the controller is able to produce a clear improvement in the Total Harmonic Distortion with up to a 30 times improvement compared to open-loop with a clear reduction in the noise. This places the audio quality on pair with current solutions.

0 Introduction

During the last decade, switch-mode audio amplifiers have become a common choice for audio applications. This is due to the superior efficiency these amplifiers offer compared to other traditional linear amplifiers. With efficiencies in the vicinity of 90% [1, 2], the achievements of high power density systems is possible. In terms of linearity, switch-mode amplifiers have shown great performance with Total Harmonic Distortion as low as 0.001%, [3, 4, 5]. The switch-mode power amplifier works by modulating the input audio into a high frequency level discrete signal which drives a power stage. The modulation process of the signal is one of the primary sources of distortion due to the non-linearities in the process [3, 6, 7]. Another source of distortion is the power stage [8, 9]. The power stage is connected directly to the supply voltage which results in disturbances in the supply voltage being reflected in the audio. To prevent these disturbances and non-linearities from introducing excessive distortion and noise to the amplified audio signal, the principals of feedback and control theory have been utilized to correct and suppress the unwanted behaviours of the switch-mode power amplifier.

To this day the majority of switch-mode power amplifiers have been using the principals of classical control due to its straight forward theory and the ease of implementing it in Single Input Single Output (SISO) systems [10, 11]. However, limitations in the theory often result in the control solution being only sub-optimal. Depending on the system, the limitations of the method can be so severe that no satisfactory solution can be obtained. This can in audio applications result in less reduction of distortion and noise than what is possible. One way to address this is through the means of modern control theory. Modern control, unlike output control, considers all the states of the system hence allowing for very precise control of the dynamics.

In this paper the principles of state space modelling, and how it can be used in conjunction with class-D amplifiers, is shown. Modern control theory methods will be applied to design and simulate a full state feedback integrating controller for use with a high frequency bridge tied class-D amplifier. The benefits and drawbacks of using modern control for class-D amplifiers will be discussed. Finally, measured results obtained from an implemented test board will be presented to support the simulations.

1 State Space Average Modelling

The state space average model is a special case of state space modelling which is used to describe piecewise continuous systems such as Switch Mode Power Supply (SMPS). Here the method has been widely used since it provides an internal model of the system thus making it suitable for describing the small signal transfer properties of the system [12, 13, 14]. The state space average model works by modelling all the states, a system can assume during a switching

*Nicolai Dahl, nicolai@jerram.dk

period, separately. The models are then averaged with a weighted average based on the duty cycle that corresponds to the chosen linearization point. The duty cycle represents the percentage of time in a switching period where the level discrete signal of the modulator will be high.

1.1 Filter Transformation

For a class-D amplifier with a bridge tied load (Figure 1a) the system can take two states assuming the dead time can be neglected. This will give the following outputs from the power stage to the output filter:

$$V_{sw+} = \begin{cases} V_{cc} & \forall dT_{sw} \\ 0 & \forall \bar{d}T_{sw} \end{cases}$$
$$V_{sw-} = \begin{cases} 0 & \forall dT_{sw} \\ V_{cc} & \forall \bar{d}T_{sw} \end{cases} \tag{1}$$

Where V_{sw+} and V_{sw-} are the differential output pair, d is the duty cycle, V_{cc} is the supply voltage for the power stage and T_{sw} is the time of the switching period. The differential nature of the bridge tied amplifier will increase the model complexity due to the existence of more internal states compared to a single ended configuration. To keep the model complexity to a minimum, the symmetry of the differential design is utilized to transform the system into a single ended equivalent system by using the methods presented in [15]. Figure 1a shows the differential filter and 1b its single ended equivalent with the necessary scaling of component values to achieve the same filter properties as the differential filter. Here C_{BTL} and R_{BTL} are the capacitance and load for the bridge tied system which changes value when transformed.

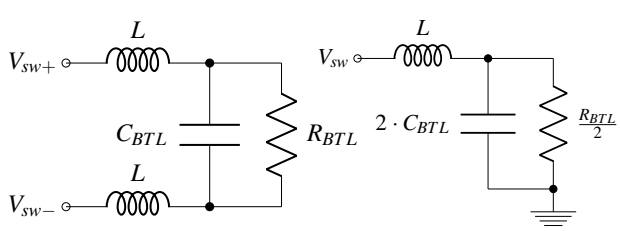

(a) Differential Filter (b) Single Ended Filter

Fig. 1: Transformation from differential to single ended filter

The filter transformation further simplifies the outputs from the power stage to the output filter to be a single output which is symmetric around the reference voltage. Equation 2 shows the transformed output.

$$V_{sw} = \begin{cases} V_{cc} & \forall dT_{sw} \\ -V_{cc} & \forall \bar{d}T_{sw} \end{cases} \tag{2}$$

Since audio is an AC signal, the linearization point is set to be the reference voltage where the duty cycle is $d = 0.5$. This leads to the state space average model being identical to a standard state space model which will be used to describe the system. Equation 3 shows the standard form of a state space model for a Linear Time Invariant (LTI) system.

$$\dot{x}(t) = Ax(t) + Bu(t)$$
$$y(t) = Cx(t) + Du(t) \tag{3}$$

1.2 State Space Model

In general it is desired to model all the internal states since it will provide the most accurate description of the system. However, when designing an analog full state controller only the internal states that are directly measurable are of interest. This is because the full state controller must have a feedback path for every state which makes it crucial that the state is accessible [16]. In theory an observer could be implemented to model the states that are not directly measurable but in practice it would be too unpractical to implement an analog observer. If digital control is used instead a more comprehensive description of the amplifier and loudspeaker can be made through state estimation. However, loudspeakers are very non-linear in the operational region thus adaptive methods [17] or more linear magnet-only loudspeakers [18] should be considered for the best results. This, however, is out of the scope of this paper.
The directly measurable states in the class-D amplifier are: The speaker voltage V_{spk}, the speaker current I_{spk} and the inductor current I_{ind}. All three states are included in the state vector $x(t)$ (eq. 4).

$$x(t) = \begin{bmatrix} I_{ind} \\ I_{spk} \\ V_{spk} \end{bmatrix} \tag{4}$$

The output filter of the amplifier is a 2nd order low pass filter, thus only two states are needed to describe it (V_{spk} and I_{ind}). The inclusion of a third state (I_{spk}) makes it possible to model the speaker as a resistor and an inductor in series. Here the inductor represent the self-inductance of the voice coil of the loudspeaker thus increasing the model order of the speaker from a 0th order to a 1st order model. Figure 2 shows the modelled circuit.

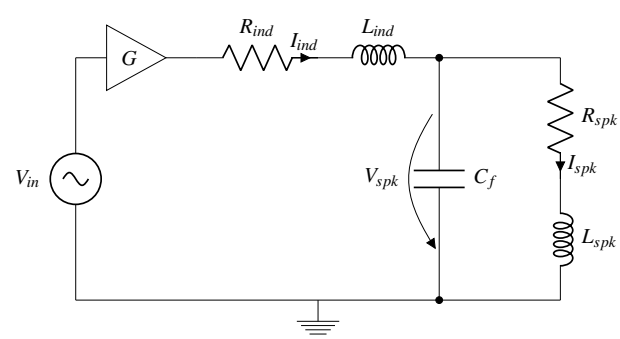

Fig. 2: The circuit modelled in the state space model

Here G is the gain through the modulator and the power stage. Equation 5 provides an approximative gain through the amplifier based on the voltage amplification and the desired maximum modulation index M_{max}.

$$G = \frac{V_{spk}}{V_{in}} \cdot M_{max} \tag{5}$$

The input to the state space model $u(t)$ is in this case the audio input $V_{in}(t)$. From this the system matrix A (eq. 6) and the input matrix B becomes:

$$A = \begin{bmatrix} -\frac{R_{ind}}{L_{ind}} & 0 & -\frac{1}{L_{ind}} \\ 0 & -\frac{R_{spk}}{L_{spk}} & \frac{1}{L_{spk}} \\ \frac{1}{C_f} & -\frac{1}{C_f} & 0 \end{bmatrix} \quad B = \begin{bmatrix} \frac{G}{L_{ind}} \\ 0 \\ 0 \end{bmatrix} \tag{6}$$

The output of the system is selected to be the voltage across the speaker for convenience. The output could also be the current through the speaker. This would give a better control of the speaker dynamics but also increase the requirements for the accuracy of the self-inductance of the voice coil thus making the amplifier less acceptable for different speakers. Based on the selected output the output matrix C and feed through matrix D becomes:

$$C = \begin{bmatrix} 0 & 0 & 1 \end{bmatrix} \qquad D = 0 \tag{7}$$

With the linear state space model constructed, component values can be assigned. The supplied class-D amplifier will have component values which ensures that the specifications in table 1 are met. The amplifier will be tested into a resistive load hence the inductance of the load is assumed to be close to zero and is estimated to be 2 nH. Doing the filter transformation will result in the system and input matrix (Eq. 8).

Cutoff Frq (f_c)	155	kHz
Quality Factor (Q)	4.5	
Idle Switch Frq (f_{sw})	1.9	MHz
Max Modulation Index (M_{max})	76	%
Input Voltage pk-pk (V_{in})	2	V
Gain (G)	19.2	dB
Max Output Power (P_{rms})	9	W
Load Resistance (R_{spk})	8	Ω
Load Inductance (L_{spk})	2	nH

Table 1: Class-D Amplifier Specifications

$$A = \begin{bmatrix} -\frac{37\text{m}\Omega}{1\mu\text{H}} & 0 & -\frac{1}{1\mu\text{H}} \\ 0 & -\frac{4\Omega}{1\text{nH}} & \frac{1}{1\text{nH}} \\ \frac{1}{1.32\mu\text{F}} & -\frac{1}{1.32\mu\text{F}} & 0 \end{bmatrix} \quad B = \begin{bmatrix} \frac{9.12}{1\mu\text{H}} \\ 0 \\ 0 \end{bmatrix} \tag{8}$$

2 Open-loop System Response

The found values allow for an analysis of the open-loop system response. Figure 3 shows the bode plot of the open-loop system. Here it is seen that the frequency response follows the response of an underdamped 2nd order low pass filter. The underdamping results in a large resonance peak, 13 dB higher than DC, at the natural frequency (138.6 kHz). This is typically unwanted in a class-D amplifier since the damped oscillation it creates, impedes the ability to improve the fidelity when using classical control since an increase in the gain at the resonance frequency will also increase the resonance. However, in modern control, this problem is easily solved, and thus the resonance peak can be used to improve the distribution of heat in the power stage by moving losses from the switching devices to the filter [19].

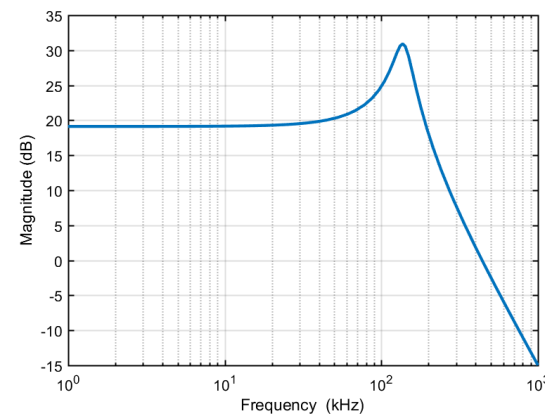

Fig. 3: Calculated open-loop bode plot

To get a better understanding of the amount of oscillation produced from the resonance peak, a step response is conducted. Figure 4 shows the step response of the open-loop system. Here it is clear that the oscillation generates extensive overshoots (70.4 %) and settles to within 2 % of the final value in 40.3 μs. Both of these properties must be reduced to improve the response of the system.

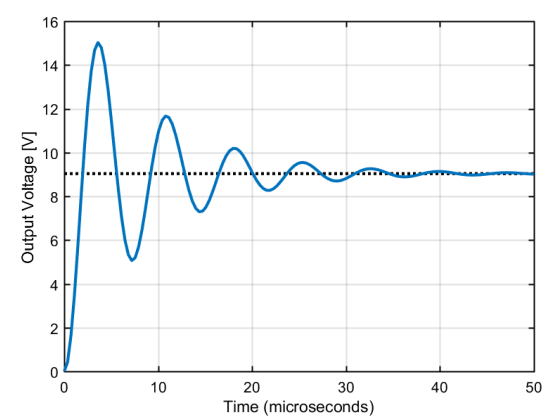

Fig. 4: Calculated open-loop step response

3 Controller Design

3.1 Controllability

One requirement must be fulfilled when designing a full state controller. This is the need for the important states of the system to be controllable. A state is controllable when the state can be affected by the input of the system. If a

state is not controllable it must at least be stabilizable such that the state will not diverge over time. To investigate the controllability, the controllability matrix, which consists of multiple combinations of the system matrix and input matrix, is used [16]. From the controllability matrix the amount of controllable states can be determined based on the rank of the matrix. If the rank is full all states are controllable. Matrix 9 shows the controllability matrix for the class-D amplifier system and equation 10 the resulting rank.

$$M_c = \begin{bmatrix} B & AB & A^2B \end{bmatrix} = \begin{bmatrix} -\frac{G}{L_{ind}} & -\frac{G \cdot R_{nd}}{L_{ind}^2} & -\frac{G \cdot (L_{ind} - C \cdot R_{ind}^2)}{C \cdot L_{ind}^3} \\ 0 & 0 & \frac{G}{C \cdot L_{spk} \cdot L_{ind}} \\ 0 & \frac{G}{C \cdot L_{ind}} & -\frac{G \cdot R_{ind}}{C \cdot L_{ind}^2} \end{bmatrix} \tag{9}$$

$$\text{Rank}(M_c) = 3 \tag{10}$$

Since all the states are proven controllable, the methods for designing a full state integral controller can be applied.

3.2 Integral Transformation

Due to the non-linearities in the class-D amplifier coming from the modulator and output filter an integration term is desirable. The integration term is added to improves the tracking capabilities such that the class-D amplifier to a certain extend maintains:

$$V_{spk} \propto V_{in} \quad \forall V_{in} \subseteq V_{span} \tag{11}$$

Where V_{span} is the chosen range of input voltage the amplifier can take without clipping. This property is especially useful when the controller is used in the actual implementation since it counteracts the non-linear behaviours. The integration term will result in an I controller for the error signal $e(t)$, and thus be in series with the class-D amplifier. Because of this, it is essential that the time constant for the integrator will result in a bandwidth greater than the bandwidth of the signal into the system to ensure proper tracking. For the class-D amplifier, this means that the bandwidth of the integrator should be so high that audio content can pass through it without being attenuated. Audio is present within 20 Hz to 20 kHz. Thus the integrator will easily be able to meet this requirement due to the cutoff frequency of the output filter being at 155 kHz, providing plenty of bandwidth to work with.

To include the integrator term into the state space model, an integral transformation is applied:

$$A_i = \begin{bmatrix} A & 0 \\ -C & 0 \end{bmatrix}, \quad B_i = \begin{bmatrix} B \\ 0 \end{bmatrix}, \quad C_i = \begin{bmatrix} C & 0 \end{bmatrix} \tag{12}$$

This results in an extra state for the integrator (q) in the state space model, hence the new state vector becomes:

$$x(t) = \begin{bmatrix} I_{ind} \\ I_{spk} \\ V_{spk} \\ q \end{bmatrix} \tag{13}$$

The integration state q simply consist of the negative output of the system which in this case is $-V_{spk}$. This is used as the negative feedback to generate the error signal for the I controller. With the integrator transform done, the Linear Quadratic Regulator design approach can be applied to the system [20, 16].

3.3 Linear Quadratic Regulator

The Linear Quadratic Regulator (LQR) is an optimization method used in modern control to find the optimal full state controller with time varying gains. However, time varying gains are often not practical nor necessary hence a simplified steady state LQR method has been developed which will be used for the system. This method optimizes a cost function with the mostly used cost function being the following quadratic performance index [20, 16]:

$$J(u) = \lim_{t \to \infty} \int_0^t x^T(t) R_1 x(t) + u(t)^T R_2 u(t) \, \mathrm{dt} \tag{14}$$

Here $x(t)$ is the states of the system and $u(t)$ the control signal to the system. R_1 and R_2 are penalty matrices which are used to emphasize the performance of specific states and control signals. It is desired to minimize the index $J(u)$ in equation 14.

$$\min J(u) \qquad \text{s.t.} \quad \dot{x}(t) = A_i x(t) + B_i u(t) \tag{15}$$

This can only be solved numerically for non-linear systems which easily becomes very time consuming. By using a linearized state space model this is avoided and static optimization can be used to find optimal steady state gains for the full state feedback controller. It can be shown that the limiting constant solution P_∞ to the performance index can be found by solving the Algebraic Riccati Equation (eq. 16) [16].

$$0 = A^T P_\infty + P_\infty A + R_1 - P_\infty B R_2^{-1} B^T P_\infty \tag{16}$$

From this the optimal constant gains for the full state controller become:

$$K_\infty = R_2^{-1} B^T P_\infty \tag{17}$$

For the class-D amplifier it is desired to compensate for any non-linearities as fast as possible and to reduce the damped oscillation on the output. To realize this, the penalty matrix R_1 is designed to heavily penalize the integration state. This will move the pole of the integrator to the left in the s-plane and make it settle somewhere close to the poles of the 2nd order filter, thus making the time constant of the integrator about the same as the output filters. The matrices in 18 shows the placement of the poles before and after the controller is applied.

$$\begin{bmatrix} 0 \\ -4\cdot 10^9 \\ -1.13\cdot 10^5 + 8.67i\cdot 10^5 \\ -1.13\cdot 10^5 - 8.67i\cdot 10^5 \end{bmatrix} \rightarrow \begin{bmatrix} -5.14\cdot 10^5 \\ -4\cdot 10^9 \\ -6.62\cdot 10^5 + 5.82i\cdot 10^5 \\ -6.62\cdot 10^5 - 5.82i\cdot 10^5 \end{bmatrix} \tag{18}$$

Since the damped oscillation limits the movement of the integrator, it is to be expected that the LQR will further increase the damping of the output filter such that the oscillation will be reduced. All these pole movements generate a growth in the control signal which is limited by the supply voltage. It is important that the control signal does not clip since this would result in the system acting as an open-loop system. To avoid this, the penalty matrix R_2 is increased to emphasize the size of the control signal thereby reducing it. Equation 19 shows the two penalty matrices. Both matrices are found through hand-tuning of the different penalties.

$$R_1 = \begin{bmatrix} 0.7 & 0 & 0 & 0 \\ 0 & 10^{-3} & 0 & 0 \\ 0 & 0 & 10^{-3} & 0 \\ 0 & 0 & 0 & 10^{11} \end{bmatrix}, \quad R_2 = 30 \tag{19}$$

By providing a small penalty to the inductor current, the in-rush current is limited thus eliminating any overshoot at the output. Using the obtained model in 12 and the penalty matrices in 19 the feedback gains are found using equation 16 and 17. The resulting gains are shown in 20. Here it is particularly noticeable that the state, describing the current through the speaker, is of next to no interest for the controller. This is probably because the controller focusses on controlling the voltage across the speaker and since the speaker current is a result of the voltage across the speaker, the current does not matter for the control of the amplifier.

$$\begin{aligned} K_\infty &= \begin{bmatrix} K_{ind_I} & K_{spk_I} & K_{spk_V} & -K_i \end{bmatrix} \\ &= \begin{bmatrix} 0.177 & -1.062\cdot 10^{-5} & 0.056 & -5.774\cdot 10^4 \end{bmatrix} \end{aligned} \tag{20}$$

In equation 20 the last gain is the negative inverse of the time constant of the integrator, thus the time constant becomes:

$$\tau_i = \frac{1}{-K_i} = 17.321\mu s \tag{21}$$

With the feedback gains and the time constant found, the loop can be closed according to the closed system shown in figure 5.

An analysis of the closed-loop system can be conducted. Figure 6a shows the frequency response and figure 6b the step response of both the open-loop and the closed-loop system.

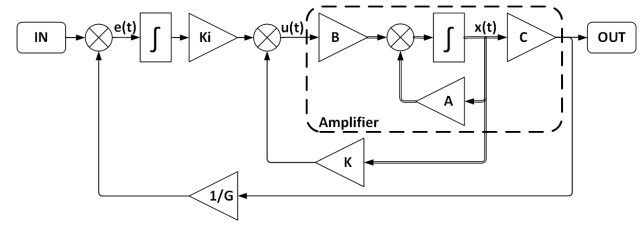

Fig. 5: Amplifier with control. The gain block K consists of the first three elements of K_∞ where each gain is assigned to each state of the amplifier. The last gain in K_∞ is placed after the integrator to set the time constant.

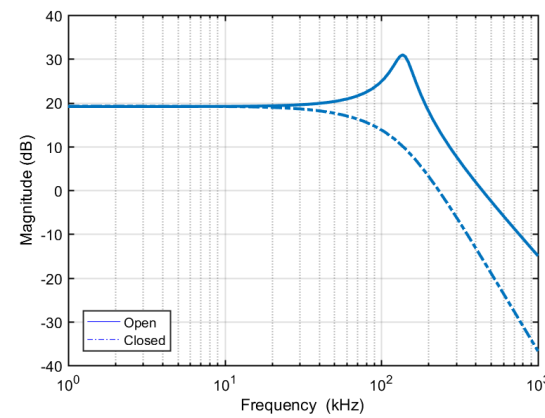

(a) Frequency Response

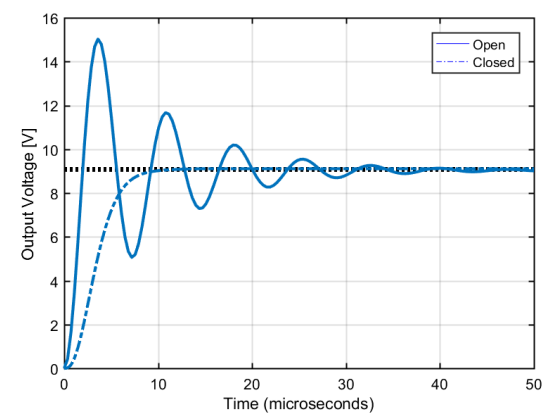

(b) Step Response

Fig. 6: Calculated open and closed-loop step and frequency response for the amplifier

The bode plot clearly shows that the damping of the complex conjugated pole pair has been increased since the resonance peak from the open-loop response has completely disappeared. The cutoff frequency of the integrator has moved to approximately 83.8 kHz giving a total bandwidth of the system of 71.3 kHz. This is below the cutoff frequency of the 2nd order filter but still around 3.5 times faster than the minimum requirement for audio at 20 kHz. The step response further confirms that the resonance peak has been eliminated. This can be seen in the closed-loop response which does not have any overshoot or ringing. The step has a rise time of 4.8 μs and a settling time of 8.8 μs.

In order to know the behaviour of the remaining states, a simulation of the linear model is made. Figure 7 shows all the states of the closed-loop system.

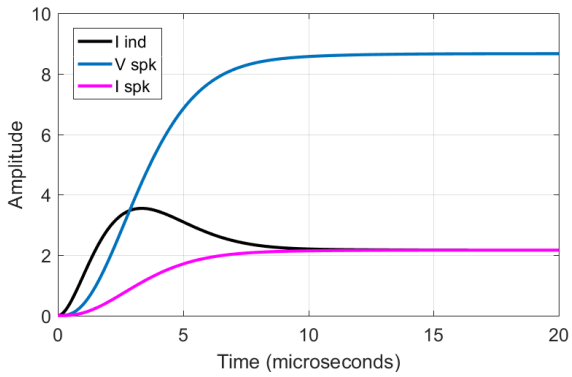

Fig. 7: Calculated step responses for all states

Looking at the states, it is seen that the current through the inductor reaches almost 4 A when the step is conducted. This current peak is of no concern because of two reasons. First, the step is made on a single ended model. This results in the speaker resistance only being half of the size it will be in the full bridge due to the conversion made in section 1.1. Due to the reduced resistance size, the current in the model is doubled compared to the implementation. Because of this it is important to remember that the feedback gains for the states that describe the currents should be the double of what has been found in equation 20. Secondly, the steps conducted are absolute worst case scenarios. In practice, audio would never make an instantaneous step, thus the overshoot of the current through the inductor would never happen to such extends. The reason why the steps are used are to guarantee robustness of the controller design. If the step response is stable a response to a sinusoid is also guaranteed to be stable.

4 Switching Model

To investigate if a switching system will act in the same manner as the linearized system just derived, a non-linear switching Simulink model has been made. This model have the same specifications and component values as the linearized model found in table 1 and equation 8. The switching model implements an AIM modulator [21, 22], propagation delay, dead-time and non-ideal behaviours of the operational amplifiers. These expansions are made to account for the switching behaviour of the system and to determine how switching residuals will affect the controller. Further, the switching model includes a first order low pass filter at the control signal with a cutoff frequency of 550 kHz. The purpose of the filter is to filter out the remaining switching residuals before the control signal enters the modulator without adding additional phase in the audio band. Figure 9 shows the described Simulink model.

To ensure the equality of the models, an identical step of the open-loop (figure 8a) and the closed-loop (figure 8b) are conducted for both models.

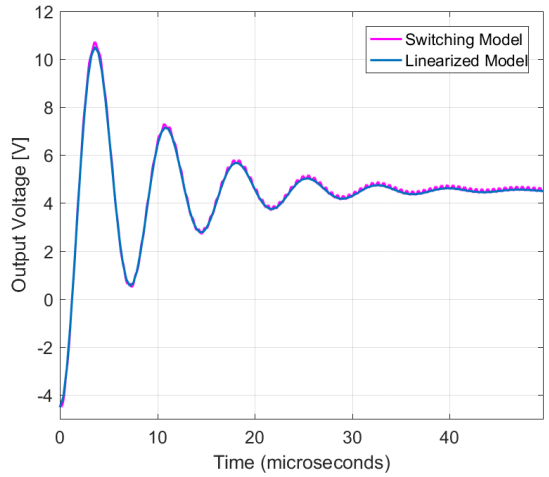

(a) Open-loop

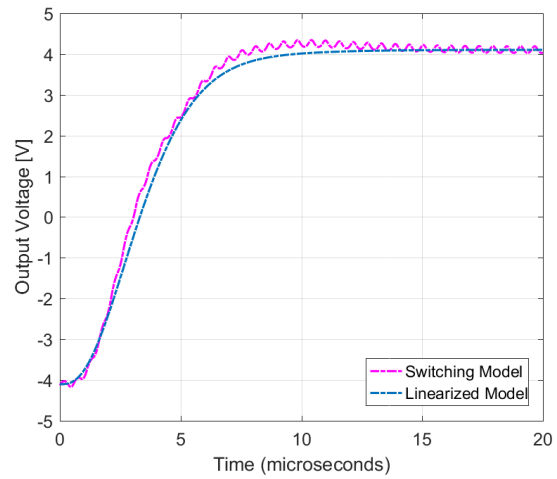

(b) Closed-loop

Fig. 8: Open and closed-loop step response for the linearized state space model and the switching simulation

Figure 8a clearly shows an identical behaviour of the state space model and the switching Simulink model when in open-loop. Here the voltage ripple from the switching is almost non-existing due to the resonance from the filter dominating the signal. On figure 8b the switching model overshoots slightly due to the non-ideal behaviour of the operational amplifiers. This time, the voltage ripple from the switching is also more visible because the resonance has been eliminated.

These results confirm that a switching system such as a class-D amplifier will follow the same behaviour as the linear state space system.

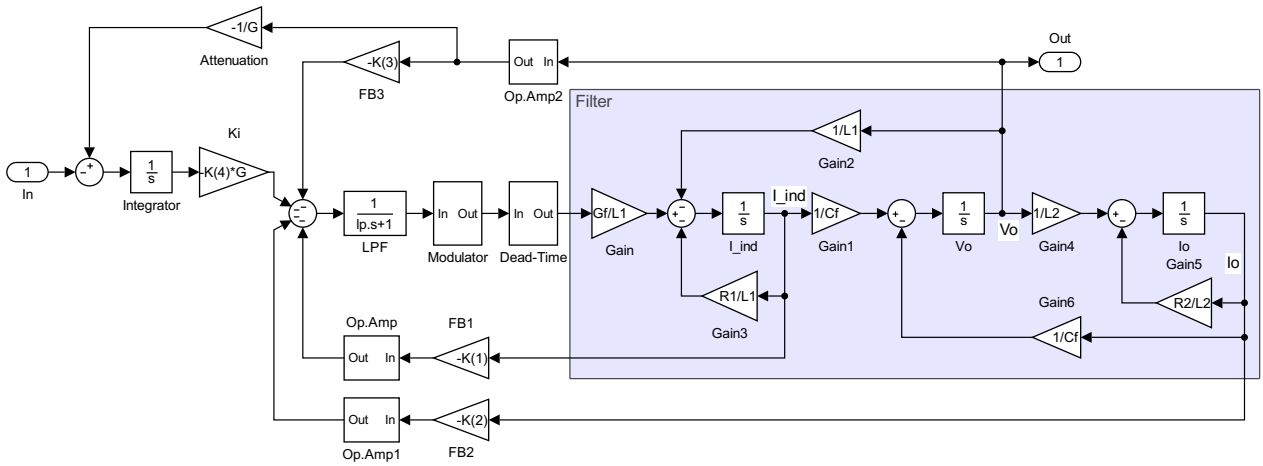

Fig. 9: Simulink model used for simulating the switching behaviour of the system

5 Implementation

To assess the true performance of the system with the designed controller a physical implementation is made. The implementation is a 12V full-bridge class-D amplifier made with the same values as used for the switching and linearized model. The implementation also implements the filter at the controller used in the switching model. Figure 10 shows a picture of the physical implementation.

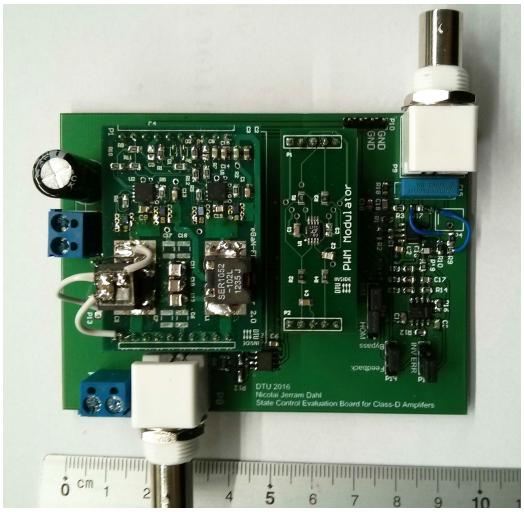

Fig. 10: Prototype of the class-D amplifier and control loop

In the implementation, the current in the inductor is measured using a lossless equivalent time constant method as proposed in [23, 24]. This method is used since it has a minimal impact on the filter characteristics and has no current sense resistor thus avoiding the resistive loss. For the speaker current, the traditional resistor method is used to measure the current. The physical implementation is compared to the results obtained in figure 8 by conducting the same step on the input in open and closed-loop. The implementation is tested into an 8 Ohm resistor. Thus the inductance of the load is assumed to be close to zero. Figure 11a shows the step response of all the systems.

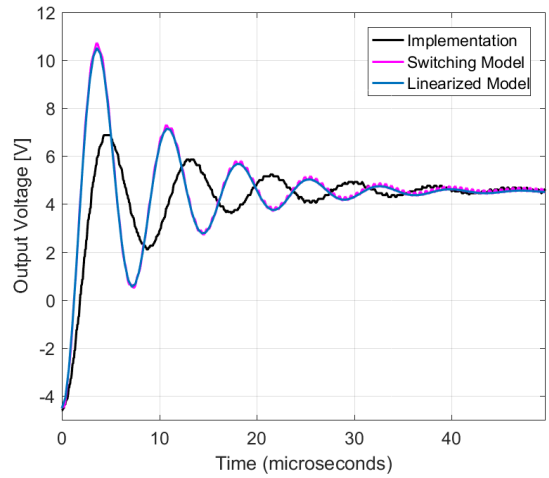

(a) Open-loop

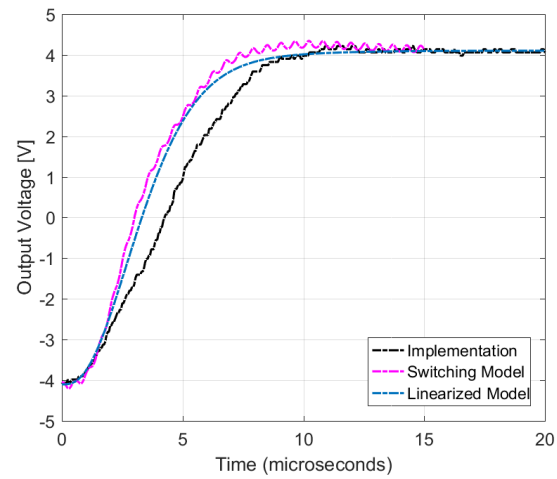

(b) Closed-loop

Fig. 11: Open and closed-loop step response for the physical implementation, the linearized and switching simulation

From the step response in figure 11a it can be seen that the measured step of the implementation deviates slightly from the models. The implementation shows both more damping and an oscillation at a slightly lower frequency. The reason for this deviation is probably because the Equivalent Series Resistance (ESR) of the capacitors in the output filter have not been modelled in the models. The ESR takes energy out of the system thus reducing the overshoot. Since the implementation has more damping than the models, it would be possible to design a controller which is able to track harder than what is possible with the models. This is because the increased damping of the system results in less control effort to move the poles of the filter, thus more control effort could be dedicated to the speed of the integrator.

6 Results

Figure 11b shows the closed-loop step response of the implementation and the models. The implementation reaches the final value at the same time as the models but with a slightly different trajectory. The difference in the trajectory is due to the ESR in the capacitor which results in a slightly slower response than expected. However, since the final value is reached at the same time, the difference in the trajectory only has a small impact on the performance.

Measurements of the Total Harmonic Distortion plus Noise (THD+N) determine the performance of the system when playing audio. Figure 12a to 12c shows the measured THD+N for the physical implementation for the three frequencies: 100 Hz, 1 kHz and 6.6 kHz, with and without the controller connected. The frequency 6.6 kHz provides a worst-case THD measurement as it is the highest frequency before the third harmonic falls out of the audio spectrum. At low power, where the noise is dominant, the closed-loop is able to suppress the noise better than the open-loop due to the control structure reducing the noise variance. Figure 12d presents the THD+N for the three closed-loop measurements. Here it is seen that the THD+N measurements at 1 kHz and 6.6 kHz are decreasing until 0.01 W where the non-linearities starts to become dominant. The 100 Hz THD+N measurement is able to decrease until 1.5 W, where clipping starts to occur. The reason for the improved THD+N at 100 Hz is the larger bandwidth available resulting in the integrator being able to suppress the non-linearities more. Overall the closed-loop THD+N measurements consistently reach down to 0.02% and below 0.01% for the 100 Hz measurement yielding up to a 30 times improvement in the THD+N compared to open-loop. These results place this solution on pair with state-of-the-art such as [25, 26] from 2012 and 2016. In [25] THD+N measurements down to just below 0.02% at 1 kHz and 0.08% at 6.6 kHz were obtained. In [26] the obtained THD+N measurements go down to 0.01% at 1 kHz and fluctuates around 0.06% at 6.6 kHz. Thus the presented amplifier delivers similar THD+N at 1 kHz, but noticeable lower and more consistent THD+N results at 6.6 kHz.

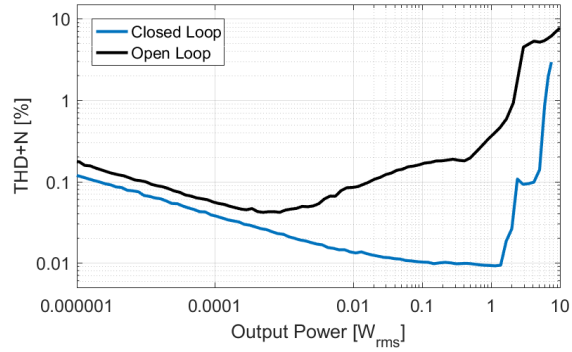

(a) 100 Hz

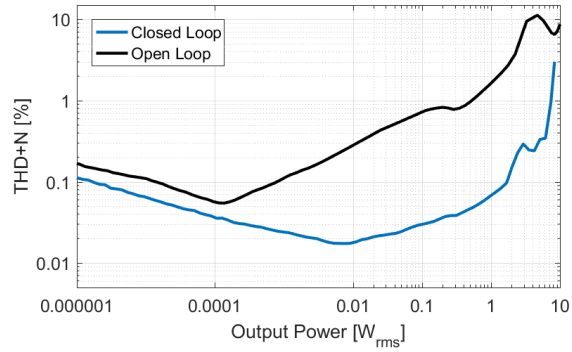

(b) 1 kHz

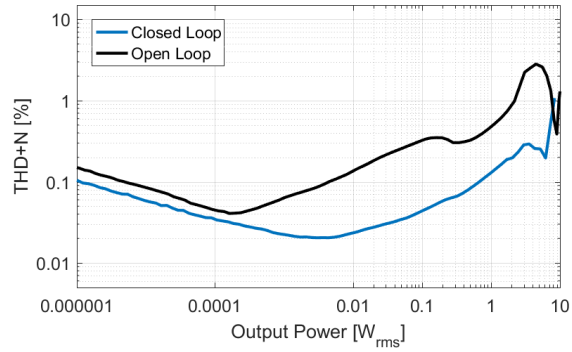

(c) 6.6 kHz

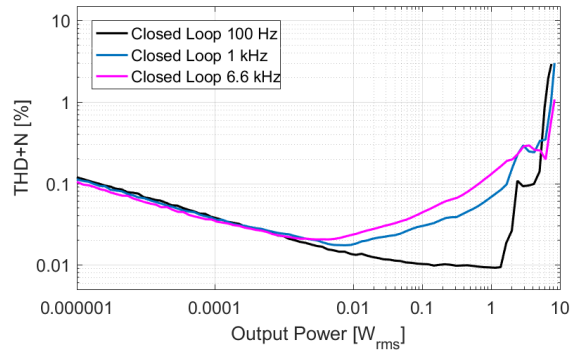

(d) All closed-loop measurements

Fig. 12: THD+N vs. Output power measured on the implemented amplifier for the three frequencies: 100 Hz, 1 kHz and 6.6 kHz

7 Conclusion

This paper presented the fundamentals of modern control and used them in conjunction with class-D amplifiers. Here filter transformation and state space modelling were used to construct a linear model of a high frequency class-D amplifier with a large resonance peak. An optimal linear full state integral controller based on the state space model was designed, using the LQR method, and verified on a linear and switching model. Finally, measurements on a class-D amplifier with the implemented controller showed step responses and THD+N measurements which aligned well with the theory. The THD+N measurements showed an overall improvement with up to 30 times reduction in the THD+N compared to the amplifier without the controller as well as lower noise through the amplifier. The results obtained are on pair with current solutions with an overall improvement in the THD+N at 6.6 kHz. This proves that the principals of modern control achieve good performance in class-D amplifiers, even when the output filter has a large resonance.

8 Future Work

The integration term needs to be heavily emphasized in the penalty matrix to acquire the desired gain and response of the amplifier. This results in a large control effort which gets limited by the possible output swing of the operational amplifiers and the input range of the modulator. Thus, investigation of alternative cost functions for the control loop should be done to reduce the current size of the integrator as well as reducing the control effort making it more feasible to add an additional global control loop.

9 REFERENCES

[1] K. Nielsen, "Audio power amplifier techniques with energy efficient power conversion," *Technical University of Denmark, Ph. D. Thesis April* (1998).

[2] M. Duraij, N. E. Iversen, L. P. Petersen, P. Boström, "Self-oscillating 150 W switch-mode amplifier equipped with eGaN-FETs," presented at the *Audio Engineering Society Convention 139* (2015).

[3] B. Putzeys, "Simple self-oscillating class D amplifier with full output filter control," presented at the *Audio Engineering Society Convention 118* (2005).

[4] S. Poulsen, M. A. Andersen, "Simple PWM modulator topology with excellent dynamic behavior," presented at the *Applied Power Electronics Conference and Exposition, 2004. APEC'04. Nineteenth Annual IEEE*, vol. 1, pp. 486–492 (2004), https://doi.org/10.1109/APEC.2004.1295852.

[5] J. Lu, R. Gharpurey, "A self oscillating class D audio amplifier with 0.0012% THD+ N and 116.5 dB dynamic range," presented at the *Custom Integrated Circuits Conference (CICC), 2010 IEEE*, pp. 1–4 (2010), https://doi.org/10.1109/CICC.2010.5617615.

[6] N. Dahl, N. E. Iversen, A. Knott, M. A. Andersen, "Comparison of Simple Self-Oscillating PWM Modulators," presented at the *Audio Engineering Society Convention 140* (2016).

[7] S. Poulsen, M. A. E. Andersen, "Self oscillating PWM modulators, a topological comparision," presented at the *Power Modulator Symposium, 2004 and 2004 High-Voltage Workshop. Conference Record of the Twenty-Sixth International*, pp. 403–407 (2004), https://doi.org/10.1109/MODSYM.2004.1433597.

[8] R. Selva Kumar, V. Karthick, D. Arun, "A review on dead-time effects in PWM inverters and various elimination techniques," (2014).

[9] T. Ge, J. S. Chang, W. Shu, "Power supply noise in bang-bang control Class D amplifier," presented at the *Circuits and Systems, 2007. ISCAS 2007. IEEE International Symposium on*, pp. 701–704 (2007), https://doi.org/10.1109/ISCAS.2007.377905.

[10] M. C. Høyerby, M. A. Andersen, "Carrier distortion in hysteretic self-oscillating class-D audio power amplifiers: Analysis and optimization," *IEEE Transactions on Power Electronics*, vol. 24, no. 3, pp. 714–729 (2009), https://doi.org/10.1109/TPEL.2008.2007956.

[11] S.-H. Jung, N.-I. Kim, G.-H. Cho, "Class D audio power amplifier with fine hysteresis control," *Electronics Letters*, vol. 38, no. 22, pp. 1302–1303 (2002), https://doi.org/10.1049/el:20020936.

[12] W. Polivka, P. Chetty, R. Middlebrook, "State-space average modelling of converters with parasitics and storage-time modulation," presented at the *Power Electronics Specialists Conference, 1980. PESC. IEEE*, pp. 119–143 (1980), https://doi.org/10.1109/PESC.1980.7089440.

[13] C. Nwosu, M. Eng, "State-space averaged modeling of a nonideal boost converter," *The pacific journal of science and Technology*, vol. 2, no. 9, pp. 1–7 (2008).

[14] M. R. Modabbernia, F. K. Khoshkbijari, R. Fouladi, S. S. Nejati, "The State Space Average Model of Buck-Boost Switching Regulator Including all of The System Uncertainties," *International Journal on Computer Science and Engineering*, vol. 5, no. 2, p. 120 (2013).

[15] K. Chan, "Design of Differential Filter for High-Speed Signal Chains," (2010).

[16] E. Hendricks, O. Jannerup, P. H. Sørensen, *Linear systems control: deterministic and stochastic methods* (Springer Science & Business Media) (2008), https://doi.org/10.1007/978-3-540-78486-9.

[17] W. Klippel, "Adaptive Stabilization of Electrodynamic Transducers," *Journal of the Audio Engineering Society*, vol. 63, no. 3, pp. 154–160 (2015), https://doi.org/10.17743/jaes.2015.0011.

[18] B. Merit, A. Novak, "Magnet-Only Loudspeaker Magnetic Circuits: A Solution for Significantly Lower Current Distortion," *Journal of the Audio Engineering Society*, vol. 63, no. 6, pp. 463–474 (2015), https://doi.org/10.17743/jaes.2015.0051.

[19] N. E. Iversen, N. J. Dahl, A. Knott, M. A. E. Andersen, "Towards Higher Power Density Audio Amplifiers," (2017).

[20] S. A. Lindiya, K. Vijayarekha, S. Palani, "Deterministic LQR controller for dc-dc Buck converter," presented at the *Power and Energy Systems: Towards Sustainable Energy (PESTSE), 2016 Bien-*

nial International Conference on, pp. 1–6 (2016), https://doi.org/10.1109/PESTSE.2016.7516450.

[21] B. J. G. Putzeys, "Power amplifier," (2006 Sep. 26), uS Patent 7,113,038.

[22] A. Knott, G. R. Pfaffinger, M. Andersen, "A self-oscillating control scheme for a boost converter providing a controlled output current," *IEEE transactions on power electronics*, vol. 26, no. 9, pp. 2707–2723 (2011), https://doi.org/10.1109/TPEL.2011.2126600.

[23] LinFinity, "A Simple Current-Sense Technique Eliminating a Sense Resistor," (1998).

[24] H. P. Forghani-Zadeh, G. A. Rincon-Mora, "Current-sensing techniques for DC-DC converters," presented at the *Circuits and Systems, 2002. MWSCAS-2002. The 2002 45th Midwest Symposium on*, vol. 2, pp. II–II (2002), https://doi.org/10.1109/MWSCAS.2002.1186927.

[25] T. Instruments, "TPA3116D2 15-W, 30-W, 50-W Filter-Free Class-D Amplifier Family with AM Avoidance," (2012).

[26] M. Høyerby, J. K. Jakobsen, J. Midtgaard, T. H. Hansen, "A 2 x 70 W Monolithic Five-Level Class-D Audio Power Amplifier in 180 nm BCD," *IEEE Journal of Solid-State Circuits*, vol. 51, no. 12, pp. 2819–2829 (2016), https://doi.org/10.1109/JSSC.2016.2600251.

[27] N. E. Iversen, A. Knott, "Small signal loudspeaker impedance emulator," *Journal of the Audio Engineering Society*, vol. 62, no. 10, pp. 676–682 (2014), https://doi.org/10.17743/jaes.2014.0036.

[28] N. E. Iversen, A. Knott, M. A. Andersen, "Relationship between voice coil fill factor and loudspeaker efficiency," *Journal of the Audio Engineering Society*, vol. 64, no. 4, pp. 241–252 (2016), https://doi.org/10.17743/jaes.2016.0006.

THE AUTHORS

Nicolai J. Dahl

Niels Elkjær Iversen

Arnold Knott

Michael A. E. Andersen

Nicolai J. Dahl is an Electrical Engineering student at Technical University of Denmark where he started in 2013. His main focuses in his studies are: control theory, audio electronics and signal processing and he has since early 2014 continuously worked with class D amplifiers and their power supplies. Currently Nicolai is working on his M.Sc. degree specializing in control theory for automation.

●

Niels Elkjær Iversen is a Ph.D student at the electronics group at the Technical University of Denmark, Kongens Lyngby, Denmark. He received his M.Sc degree in December 2014. His research interest include electrical aspects of audio such as switch-mode power audio amplifiers, measurement techniques and transducer modelling. The Audio Engineering Society has appointed his research the "Student Technical Papers Award" on two occasions, at the 136th convention in Berlin and at the 139th convention in New York both later published in the AES Journal [27, 28].

●

Arnold Knott received the Diplom-Ingenieur (FH) degree from the University of Applied Sciences in Deggendorf, Germany, in 2004. From 2004 until 2009 he has been working with Harman/Becker Automotive Systems GmbH in Germany and USA, designing switch-mode audio power amplifiers and power supplies for automotive applications. In 2010 he earned the Ph.D. degree from the Technical University of Denmark, Kongens Lyngby, Denmark working on a research project under the title Improvement of out of band Behaviour in Switch-Mode Amplifiers and Power Supplies by their Modulation Topology. From 2010 to 2013 he was Assistant Professor and since 2013 Associate Professor at the Technical University of Denmark. His interests include switch-mode audio power amplifiers, power supplies, integrated circuit design, transducers, radio frequency electronics and electromagnetic compatibility.

●

Michael A.E. Andersen received the M.Sc.E.E. and Ph.D. degrees in power electronics from the Technical University of Denmark, Kongens Lyngby, Denmark, in 1987 and 1990, respectively. He is currently a Professor of power electronics

at the Technical University of Denmark. Since 2009, he has been Deputy Head of Department at the Department of Electrical Engineering. He is the author or coauthor of more than 200 publications. His research interests include switch-mode power supplies, piezoelectric transformers, power factor correction, and switch-mode audio power amplifiers